Mapping Urban Landscapes Along Streets Using Google Street View

Xiaojiang Li, Carlo Ratti and Ian Seiferling

Abstract City streets are a focal point of human activity in urban centers. Citizens interact with the urban environment through its streetscape and it is imperative to, not only map city streetscapes, but quantify those interactions in terms of human well-being. Researchers now have access to fully digitized representation of streetscapes through Google Street View (GSV), which captures the profile view of streetscapes and, thus, shares equivalent viewing angles with those of the citizen. These two facets—a wealth of streetscape photographs at city-scale and a shared perspective with the end user—underscore the potential of these data in street-level urban landscape mapping. In this study, we introduce two examples that demonstrate GSV as a high-quality data source for mapping street greenery and openness. First, the modified green view index, which estimates the visibility of street greenery, was applied to static GSV images in order to map the spatial distribution of street greenery. Second, GSV panoramas were used to quantify and map the openness of street canyons by applying a geometrical transformation and image classification to the panoramas. The results of these two novel applications of street-level photographic data illustrate its utility for quantifying and mapping key urban environmental features at the same viewpoint in which we, as citizens, experience the urban landscape.

Keywords Google street view · Urban landscape · Street greenery · Street openness

X. Li (✉) · C. Ratti · I. Seiferling
MIT Senseable City Lab, Cambridge, MA, USA
e-mail: xiaojian@mit.edu

X. Li
Department of Geography, University of Connecticut, Storrs, CT 06269, USA

M.P. Peterson (ed.), *Advances in Cartography and GIScience*, Lecture Notes in Geoinformation and Cartography, DOI 10.1007/978-3-319-57336-6_24

1 Introduction

The street is the basic unit of the city and a focal point of human activity, acting as the foundation for transportation and information exchange. Moreover, because cities are complex systems that integrate the physical with the social spaces (Salesses et al. 2013), streetscapes play an important role influencing social interactions. Taken together, city streets become one of the most critical urban landscape features effecting, or reflecting, people's lifestyles and physical, mental, and social well-being (Miller and Tolle 2016; Li et al. 2016). It follows that a thorough quantification and understanding of the physical streetscape (i.e., features and dynamics) would offer great utility to those investigating the urban environment, its physical social interactions, and implications on human well-being.

A variety of methods and data sources to model and measure the urban physical environment exist and are widely exploited in urban studies. For example, high spatial resolution remote sensing has been used for the study of street greenery, building height estimation, and other urban feature extractions. However, high spatial resolution remotely sensed data are not always available. In addition, the profile view of streetscapes, that people experience and see from the ground, is different from the overhead view captured in remotely sensed imagery (Yang et al. 2009; Li et al. 2015). Those differences can be overcome with manual inventories and field surveys, however in situ data collection are laborious and time-consuming (i.e., low-throughput) and are prone to sampling errors, especially when non-expert or volunteer-based (Nowak et al. 2014).

Google Street View (GSV) was launched in 2007 and differentiates itself from traditional mapping software by directly capturing the ground-level visual appearance. By stitching pictures taken in different angles together, GSV creates what feels like a seamless tour of city streets and it can give people the feeling of "being there" (Li et al. 2015). Given GSV's ground-level sampling of digital photographs, one can argue that its data is a directly suitable representation of cityscapes, perhaps more so than remotely sensed images. In addition, the GSV is produced based on industrial criteria and collected for many cities all over the world. It would be an important and promising data source for urban landscape mapping along the streets.

GSV images have been widely studied in the computer vision community. These studies include commercial entities identification (Zamir et al. 2011), 3D city modeling (Torii et al. 2009; Mičušík and Košecká 2009). Recently, GSV images were also used for urban studies, such as public open space auditing (Edwards et al. 2013; Taylor et al. 2011), neighborhood environmental auditing (Charreire et al. 2014; Rundle et al. 2011; Odgers et al. 2012; Griew et al. 2013), and quantifying public safety perception (Naik et al. 2014). While these examples highlight the diverse potential of GSV data, there are few studies using street-level photographs for cartographic purposes. Two novel applications of GSV image data are introduced here that quantify environmental features and map them in the urban physical landscape;

those being street greenery and openness of the street canyons. In doing so, we show how to make GSV data an incredibly promising tool for urban environmental studies.

2 Google Street View (GSV) Data Collection

GSV is a free online service featured in Google Maps and Google Earth that provides panoramic views from positions along city streets throughout much of the world (Fig. 1). Google provides several types of application programming interfaces (APIs) for accessing the GSV data as static images and 360° panoramas.

2.1 Collecting Static GSV Images

Through the Google Static Image API, users can request a given static GSV image with a HTTP URL by specifying the location coordinates (Google 2014). In addition, the static GSV images in different horizontal directions and vertical angles can be requested by specifying the parameters of *heading* and *pitch*, respectively. Figure 2 shows one requested static GSV image and the corresponding URL.

2.2 Collecting GSV Panoramas

In addition to static images, GSV panoramas can also be downloaded from the Google Server through the API. Figure 3 shows 26 × 13 tiles of a GSV panorama together with corresponding URLs. In these URLs, the *panoid* represents the

Fig. 1 A snapshot of Google Street View

Coordinate: http://maps.googleapis.com/maps/api/streetview?size=400x400&location=41.935,-87.80524300000002&fov=60&heading=180&pitch=0&sensor=false

Fig. 2 A GSV image and the corresponding Uniform Resource Locator (URL)

URL: http://cbk0.google.com/cbk?output=tile&panoid=8wRCFFwU8AQ-8MF0_TagWQ&zoom=5&x=5&y=3

URL: http://cbk0.google.com/cbk?output=tile&panoid=8wRCFFwU8AQ-8MF0_TagWQ&zoom=5&x=19&y=3

Pano ID: 8wRCFFwU8AQ-8MF0_TagWQ

Fig. 3 The tiles of a GSV panorama and their corresponding URLs

unique panorama ID, x and y represent the column and row number of the tile, respectively. A complete panorama includes 26 × 13 tiles, therefore, the x ranges from 0 to 25 and y ranges from 0 to 12.

In the new version of Google Street View Image API (2016), the GSV image metadata can be accessed. The following is an example of accessing the metadata of a GSV panorama.

URL: https://maps.googleapis.com/maps/api/streetview/metadata?size=400x400&location=42.354489,-71.059150&fov=90&heading=235&pitch=10&key=YOUR_API_KEY

```
Metadata of the a GSV panorama
{
"copyright" : "© 2017 Google",
"date" : "2016-10",
"location" : {
"lat" : 42.3545003,
"lng" : -71.0591524
},
"pano_id" : 8a9h88JXDZ8k6FC2mPbDkA",
"status" : "OK"
}
```

The returned metadata includes the acquisition date, coordinate of the panorama, and the panorama ID. There is a discrepancy between the input coordinate in the URL and the returned coordinate in the returned metadata. This is because the GSV image API will return a nearby panorama and the coordinate of the panorama if there is no panorama at the place the user specified.

In this study, GSV panoramas were collected in two steps. The first step is to get the metadata of GSV panoramas using coordinates as inputs. The second step is to download GSV panorama tiles from Google servers and mosaic the tiles to complete GSV panoramas.

3 Urban Landscape Quantification and Mapping

This section introduces two applications using GSV to map the distribution of street greenery and the openness of street canyons.

3.1 Mapping the Visibility of Street Greenery

As an important component of urban greenery, street greenery has long played a critical role in the urban landscapes. Other than the instrumental functions such as

urban heat island mitigation, storm-water reduction, airborne pollutant absorption, the street greenery also provides sensory functions to people. The existence of street greenery increases people's rating of streetscapes (Camacho-Cervantes et al. 2014; Balram and Dragićević 2005). Street greenery makes streets more walkable and beautiful (Li et al. 2015; Bain et al. 2012). In addition, the street greenery can also mitigate the visual intrusion of traffic, which would contribute to the walkability of streets. Assessment of the sensory functions of street greenery must be guaranteed for urban landscape management.

In situ manual inventories and remote sensing have been widely used to assess and map street greenery. The in situ survey is very time- and cost-consuming although it can measure detailed information about street greenery. Because of its virtues such as repeatability, synoptic view, and larger area coverage, remote sensing has become an important data source for assessment of urban greenery. With the emergence of new sensors such as LiDAR, that are now available at high, but sometimes feasible costs, it is possible to measure the canopy cover, canopy height, and even the volume of street greenery using high spatial resolution remotely sensed data with an acceptable margin of error. However, what people on the ground see or feel, which is influenced by the profile view of street greenery, would be very different compared with the overhead remotely sensed data (Li et al. 2015; Yang et al. 2009). Google Street View (GSV), providing street-level and profile views of urban landscapes, is a very promising data source for assessing the sensory function of street greenery. Considering the direct connection between the visibility of street greenery and human perceived greenery (Li et al. 2015), in this study, we mapped the visibility of street greenery in residential neighborhoods of Boston, Massachusetts, USA using street-level images.

In order to represent the street greenery in the residential area, three thousand sample sites were generated along the residential streets of the study area. In this study, we applied the modified green view index proposed by Li et al. (2015) to represent the distribution of street greenery.

The modified green view index is the average percentage of green vegetation in GSV images for 6 horizontal directions and 3 vertical directions at each sample site (Li et al. 2015) (Fig. 4). It was calculated using Formula (1),

$$Green\ View = \frac{\sum_{i=1}^{6}\sum_{j=1}^{3} Area_{g\_ij}}{\sum_{i=1}^{6}\sum_{j=1}^{3} Area_{t\_ij}} \times 100\,\% \tag{1}$$

where, $Area_{g\_ij}$ is the number of green pixels in a GSV image, for each camera direction and vertical angle for each sample site, and $Area_{t\_ij}$ is the total number of pixels in each of the 18 GSV images.

The method has been shown to correlate well with the percent vegetation cover in GSV images as manually delineated by a human eye (Li et al. 2015). As should be expected, those sites with large street tree canopies and more street greenery tend

to have larger modified green view index values than those with few trees or green cover (Fig. 5).

Figure 6 shows the spatial distribution of the modified green view index at the site level and the census tract level in Boston, Massachusetts. It is clear that the

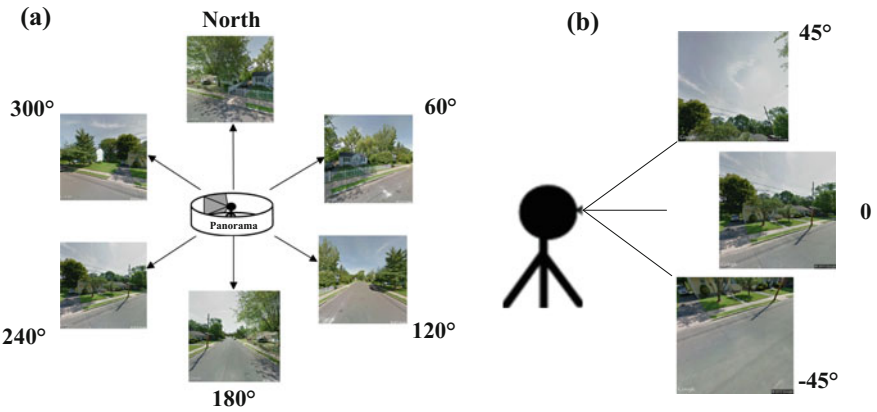

Fig. 4 GSV images of six *horizontal* directions at a sample site in the study area (**a**), and GSV images of three *vertical* view angles at a sample site (**b**)

Fig. 5 The modified green view index values in different sites of Boston

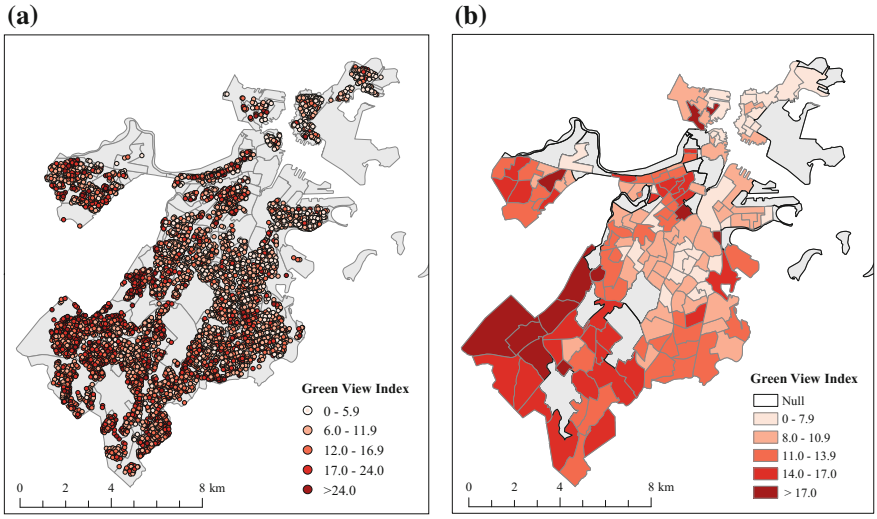

Fig. 6 The spatial distribution of the modified *green* view index in Boston, Massachusetts, (**a**) site level map, (**b**) the distribution of the *green* view index map at the census tract level

southwestern part of Boston has denser and more expansive street greenery than the northeastern part. The downtown areas of the city are characterized by low amounts of street greenery relative to the suburban areas.

3.2 Mapping the Openness of Street Canyons

The sky view factor (SVF) is a geometric quantification of the openness or the degree of sky visibility within street canyons (Oke 1981; Chapman and Thornes 2004; Ratti et al. 2002) and has a wide array of applications as an indicator of urban form, structure, and proxy of localized environmental conditions. The SVF has been applied in studies of forestry, urban climate, urbanization, air pollution, and urban heat island effects (Holmer et al. 2001; Grimmond et al. 2001; Debbage 2013; Hämmerle et al. 2011; Carrasco-Hernandez et al. 2015; Unger 2008; Eeftens et al. 2013; Chen et al. 2012; Svensson 2004; Lin et al. 2012).

The photographic method is one of the most widely used methods to estimate the SVF. However, taking fisheye images is usually required in fieldworks and the image classification is usually conducted manually. Both of these limit the photographic method to very small-scale SVF estimations. The digital surface model (DSM) simulation method is another way to estimate the SVF. In the simulation method, SVF values can be estimated based on the simulation of the light radiation in the DSM. However, the DSM is not always available and it is difficult to simulate the obstruction of tree canopies. In addition, the accuracy of SVF estimation result

is influenced heavily by the spatial resolution of the DSM. Due to these limitations and discrepancies between methods, there still exists no widely used or standard method to compute the SVF at the city or regional scales.

In this study, we propose to use the publicly accessible GSV panoramas to estimate the SVF at regional scale based on geometrical transform and image classification. We collected 11,392 GSV panoramas for SVF estimation in Boston, Massachusetts. First, we created fisheye images by projecting those collected GSV panoramas from cylindrical projection to azimuthal projection. Figure 7 shows the geometric model for the transformation of cylindrical projection to azimuthal projection. The W_c and H_c are the width and height of the cylindrical panorama, so, the radius of the fisheye image should be, $r_0 = W_c/2\pi$, and the width and height of the fisheye image are W_c/π. Therefore, the center pixel of the result fisheye image (C_x, C_y) is,

$$C_x = C_y = \frac{W_c}{2\pi} \tag{2}$$

For pixel (x_f, y_f) on the result fisheye image, the corresponding pixel on the cylindrical panorama should be (x_c, y_c),

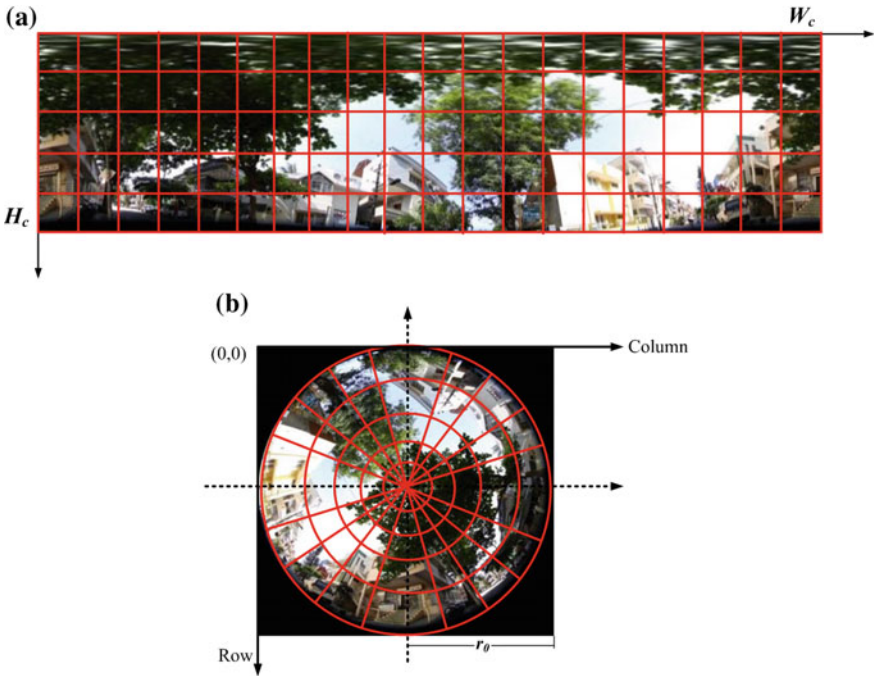

Fig. 7 Transform of cylindrical projection (**a**) to azimuthal projection (fisheye image) (**b**)

$$\begin{aligned} x_c &= \frac{\theta}{2\pi} W_c \\ y_c &= \frac{r}{r_0} H_c \end{aligned} \tag{3}$$

where, θ and r are,

$$\theta = \begin{cases} \frac{3\pi}{2} - \arctan\left(\frac{y_f - C_y}{x_f - C_x}\right), x_f < C_x \\ \frac{\pi}{2} - \arctan\left(\frac{y_f - C_y}{x_f - C_x}\right), x_f > C_x \end{cases} \tag{4}$$

$$r = \sqrt{(x_f - C_x)^2 + (y_f - C_y)^2} \tag{5}$$

Based on the geometric model between the fisheye image and the cylindrical projection GSV panorama, we further applied affine transform to generate simulated fisheye images based on the cylindrical GSV panoramas. Figure 8 shows a generated fisheye image (Fig. 8a) based on a GSV panorama (Fig. 8b).

The sky extraction is a requisite step for SVF calculation in the photographic method. In this study, an unsupervised object-based image classification method was used to extract the sky pixels from the simulated fisheye images automatically. The *meanshift* algorithm was first used to segment the fisheye images (Comaniciu and Meer 2002). The image segmentation algorithm clusters nearby pixels that have similar spectral information into objects that would enhance the difference between the sky pixels and non-sky pixels. Considering the fact that sky pixels are usually brighter than non-sky pixels, we used the overall *brightness* of pixels to differentiate the sky pixels and non-sky pixels. The *brightness* image was calculated as,

$$Brightness = (red + green + blue)/3 \tag{6}$$

where, *red*, *green*, and *blue* are the pixel values in red, green, and blue bands, respectively. Those pixels have higher *Brightness* values are sky pixels. We further used Otsu's method (Otsu 1975) to find the optimum threshold to separate the sky pixels from the non-sky pixels based on the calculated *Brightness* images. The Otsu's method chooses a global threshold automatically by minimizing the within-class variance and maximizing the between-class variance. Those pixels have their *Brightness* values higher than the threshold are sky pixels. All other pixels other than sky were treated as obstruction pixels. Figure 8c shows the classified sky pixels in a fisheye image.

Based on the sky classification results, we applied the classical photographic method to calculate the SVF. The SVF is calculated as formula (7) (Johnson and Watson, 1984),

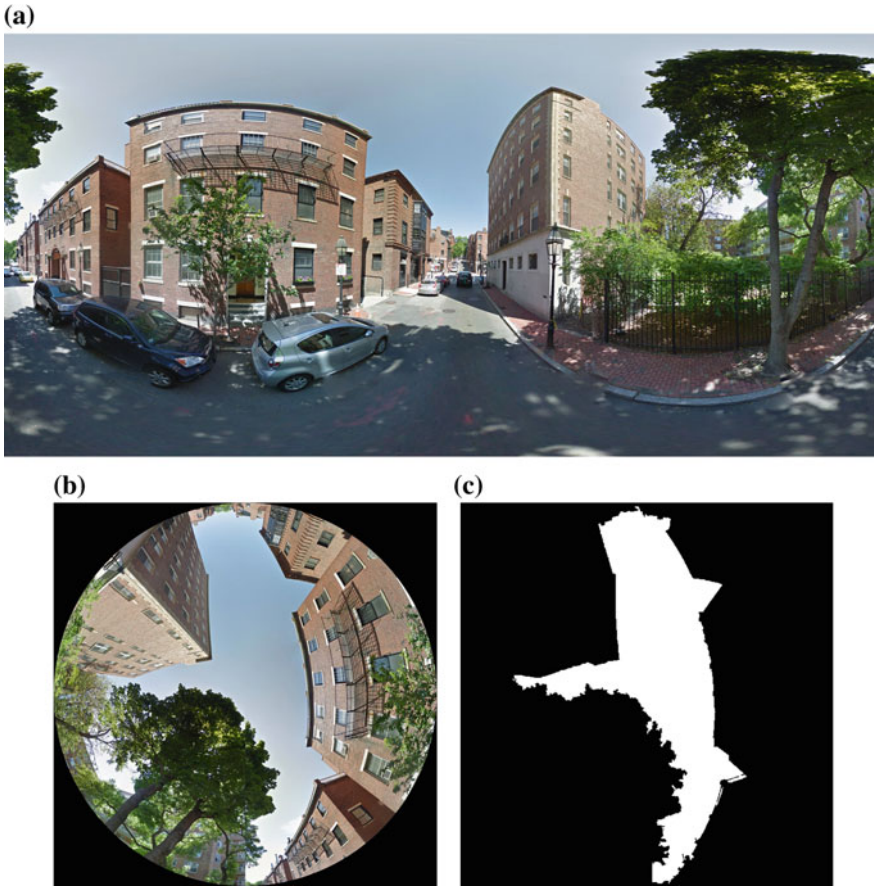

Fig. 8 GSV panorama for the SVF estimation, (**a**) a GSV panorama, (**b**) a generated fisheye image based on geometrical transform, (**c**) sky pixels classification result

$$SVF_P = \frac{1}{2\pi}\sin\left(\frac{\pi}{2n}\right)\sum_{i=1}^{n}\sin\left(\frac{\pi(2i-1)}{2n}\right)\alpha_i \tag{7}$$

where, i is the ring index, n is the number of rings (here is set to 37), and α_i is the angular width in ith ring.

By applying the above process to all retrieved GSV panoramas along the city streets, we mapped the distribution of estimated SVF values in Boston at both the point level and the census tract level (Fig. 9). It can be seen clearly that the downtown area and the southwestern part of the study area have much lower SVF values compared with other parts of the city. The SVF value is determined by the obstructions of building block and tree canopies. In the downtown area, the obstructions of high-rise buildings lead to low SVF values or relatively closed street

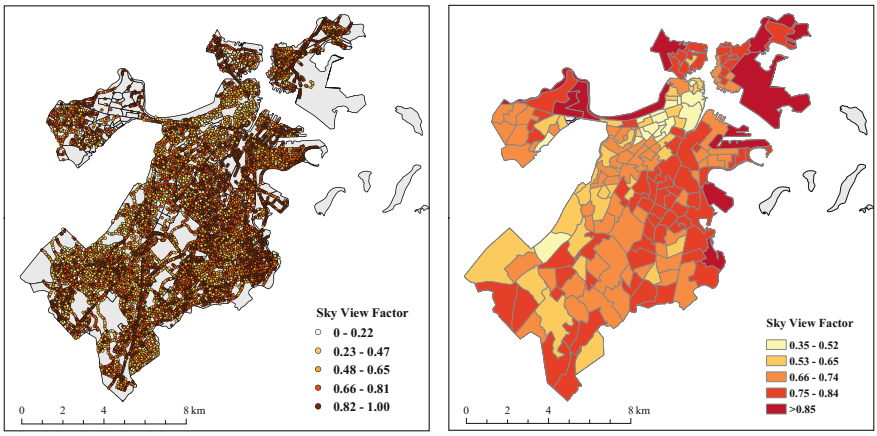

Fig. 9 The spatial distribution of the SVF values in Boston, Massachusetts

canyons. The southwestern part has much street greenery (Fig. 6), which further help contribute to the low SVF values. The street canyons in the north and southeast have higher SVF values than other regions.

4 Discussion and Conclusions

This study introduced two novel applications of publicly accessible Google Street View (GSV) images for urban streetscape mapping and characterization. Given that the street is one of the basic networks that forms cities, and one which represents a confluence of people, information and interactions, these streetscape mapping tools can contribute substantially to our understanding of the interplays between urban citizens and the built urban environment; a foundational objective al urban design and planning.

Street greenery is a critical part of the urban landscape and one that performs critical ecosystem functions and contributes directly to the health and well-being of urban citizens. There have been several metrics to measure and map urban greenness, however, few of them reflect the sensory benefits of urban greenery, not to mention achieving high spatial resolution at city-wide extents. Quantifying streetscape greenery at a ground-level perspective that is shared with the end-user (i.e., citizens) very likely captures scene information directly related to human perception and the social, economic, mental, and physical benefits that have been shown to relate to natural vegetation cover in cities. To exploit this shared perspective and take advantage of these spatially extensive data, we illustrated how one image-derived metric—the modified green view index—can provide a new

perspective to study the distribution of the street greenery. Future urban planning practices would benefit from the new index to make the cities more livable.

The openness of street canyons is an important geometrical parameter for the study of urban microclimate, air pollution migration, and human perception of the environment. Currently, a generalized and widely applied method to compute SVF in urban landscapes does not exist. Here, we demonstrated an application of GSV panoramas to, rapidly and fairly simply, estimate the street openness of Boston, Massachusetts. We have shown how a geometric transformation and simple image analysis can be used to automate a workflow to describe SVF across cities, wherein the only input is the publicly accessible GSV data. As such, the GSV-based method is suitable for large-scale SVF estimation can help researchers, urban planners and managers better understand the influence of urban form on the urban microclimate, urban air pollution migration, and human perception of urban environment.

This study has presented two example projects for the streetscape mapping in terms of the visibility of street greenery and the openness of the street canyons. The GSV data should be utilized to generate further explorations and cartographies of the urban environment. Crowdsourcing of image data and machine learning techniques will make it possible to extract additional geospatial information in cities and, both, more complex or specified metrics (e.g., proxy measures of environmental conditions like temperature, urban typologies or object mapping). For example, the *Place Pulse* project of the MIT Media lab is a seminal project to study human perception of the environment based on GSV images and crowdsourcing data collected from volunteer participants.

Although the GSV is a very promising data source for urban studies, there remain some limitations in its use for cartographic purposes. First, the sampling and resampling time inconsistency of the GSV images produce some major challenges. As it stands, GSV image coverage varies both between cities and within cities with respect to the collection dates; images within a given city may be captured at different times, in some cases, representing differing seasonal patterns (e.g., growing season vs. non-growing season months) or simply different years. Thus, at present the user must ensure a temporal standardization across their dataset if the information they are extracting can be influenced by the image capture date (e.g., seasonality of vegetation growth). In addition, the street-view is a fake 3D (Boér et al. 2013) and the GSV images were not collected for the scientific purposes. Therefore, those GSV images or panoramas would have some geometrical distortions that would potentially influence the accuracy of the mapping results. In future applications of these data, supplementary, alternative data sources should be used to validate the accuracy of the results extracted from the GSV imagery. Finally, the impact of the elevation changes was not considered in our analysis. In future studies, a local terrain model should be considered for those areas with large elevation changes.

Considering the fact that Google has now catalogued a majority of the world's cities through GSV, this publicly accessible data will play a growing role as a geospatial data source to map and measure our urban landscapes. The GSV and

other open image libraries may take on an even more significant role in areas and municipalities where geospatial data availability is an issue due to financial or accessibility constraints. In those places, GSV data has the ability to act as an important surrogate. What's more, as Google continues to update this service and library of images, it will become possible, and in fact likely very fruitful, to study and quantify the temporal changes of streetscapes in future. Recently, Google has launched a new project to using GSV cars to monitor the air pollutants. This is but one indication that the GSV collection platform will play an increasingly important role as sensor system and data source for urban environmental studies.

References

Bain, L., Gray, B., & Rodgers, D. (2012). *Living streets: Strategies for crafting public space*. New York: Wiley.

Balram, S., & Dragićević, S. (2005). Attitudes toward urban green spaces: Integrating questionnaire survey and collaborative GIS techniques to improve attitude measurements. *Landscape and Urban Planning, 71*(2), 147–162.

Boér, A., Çöltekin, A., & Clarke, K. C. (2013). An evaluation of web-based geovisualizations for different levels of abstraction and realism—What do users predict? In *International Cartographic Conference* (pp. 209–220).

Camacho-Cervantes, M., Schondube, J. E., Castillo, A., & MacGregor-Fors, I. (2014). How do people perceive urban trees? Assessing likes and dislikes in relation to the trees of a city. *Urban Ecosystem*, 1–13.

Carrasco-Hernandez, R., Smedley, A. R., & Webb, A. R. (2015). Using urban canyon geometries obtained from Google Street View for atmospheric studies: Potential applications in the calculation of street level total shortwave irradiances. *Energy and Buildings, 86,* 340–348.

Chapman, L., & Thornes, J. E. (2004). Real-time sky-view factor calculation and approximation. *Journal of Atmospheric and Oceanic Technology, 21*(5), 730–741.

Charreire, H., Mackenbach, J. D., Ouasti, M., Lakerveld, J., Compernolle, S., Ben-Rebah, M., et al. (2014). Using remote sensing to define environmental characteristics related to physical activity and dietary behaviours: A systematic review (the SPOTLIGHT project). *Health Place, 25,* 1–9.

Chen, L., Ng, E., An, X., Ren, C., Lee, M., Wang, U., et al. (2012). Sky view factor analysis of street canyons and its implications for daytime intra-urban air temperature differentials in high-rise, high-density urban areas of Hong Kong: A GIS-based simulation approach. *International Journal of Climatology, 32*(1), 121–136.

Comaniciu, D., & Meer, P. (2002). Mean shift: A robust approach toward feature space analysis. *IEEE Transactions on Pattern Analysis and Machine Intelligence, 24*(5), 603–619.

Debbage, N. (2013). Sky-view factor estimation: A case study of Athens. *Georgia. The Geographical Bulletin, 54*(1), 49.

Edwards, N., Hooper, P., Trapp, G. S., Bull, F., Boruff, B., & Giles-Corti, B. (2013). Development of a Public Open Space Desktop Auditing Tool (POSDAT): A remote sensing approach. *Applied Geography, 38,* 22–30.

Eeftens, M., Beekhuizen, J., Beelen, R., Wang, M., Vermeulen, R., Brunekreef, B., et al. (2013). Quantifying urban street configuration for improvements in air pollution models. *Atmospheric Environment, 72,* 1–9.

Google, (2014). Google Street View Image API. Retrieved October 2014, from https://developers.google.com/maps/documentation/streetview/.

Griew, P., Hillsdon, M., Foster, C., Coombes, E., Jones, A., & Wilkinson, P. (2013). Developing and testing a street audit tool using Google Street View to measure environmental supportiveness for physical activity. *International Journal of Behavioral Nutrition and Physical Activity, 10*(1), 103.

Grimmond, C. S. B., Potter, S. K., Zutter, H. N., & Souch, C. (2001). Rapid methods to estimate sky-view factors applied to urban areas. *International Journal of Climatology, 21*(7), 903–913.

Hämmerle, M., Gál, T., Unger, J., & Matzarakis, A. (2011). Comparison of models calculating the sky view factor used for urban climate investigations. *Theoretical and Applied Climatology, 105*(3–4), 521–527.

Holmer, B., Postgård, U., & Eriksson, M. (2001). Sky view factors in forest canopies calculated with IDRISI. *Theoretical and Applied Climatology, 68*(1–2), 33–40.

Johnson, G. T., & Watson, I. D. (1984). The determination of view-factors in urban canyons. *Journal of Climate and Applied Meteorology, 23*(2), 329–335.

Li, X., Zhang, C., Li, W., & Kuzovkina, Y. A. (2016). Environmental inequities in terms of different types of urban greenery in Hartford, Connecticut. *Urban Forestry & Urban Greening*, *18*, 163–172.

Li, X., Zhang, C., Li, W., Ricard, R., Meng, Q., & Zhang, W. (2015). Assessing street-level urban greenery using Google Street View and a modified green view index. *Urban Forestry & Urban Greening, 14*(3), 675–685.

Lin, T. P., Tsai, K. T., Hwang, R. L., & Matzarakis, A. (2012). Quantification of the effect of thermal indices and sky view factor on park attendance. *Landscape and Urban Planning, 107* (2), 137–146.

Mičušík, B., & Košecká, J. (2009). Piecewise planar city 3D modeling from street view panoramic sequences. In *IEEE Conference on Computer Vision and Pattern Recognition, 2009. CVPR 2009* (pp. 2906–2912). IEEE.

Miller, H. J., & Tolle, K. (2016). Big data for healthy cities: Using location-aware technologies, open data and 3D urban models to design healthier built environments. *Built Environment, 42* (3), 441–456.

Naik, N., Philipoom, J., Raskar, R., & Hidalgo, C. (2014). Streetscore-predicting the perceived safety of one million streetscapes. In *Proceedings of the IEEE Conference on Computer Vision and Pattern Recognition Workshops* (pp. 779–785).

Nowak, D. J., Hirabayashi, S., Bodine, A., & Greenfield, E. (2014). Tree and forest effects on air quality and human health in the United States. *Environmental Pollution, 193,* 119–129.

Odgers, C. L., Caspi, A., Bates, C. J., Sampson, R. J., & Moffitt, T. E. (2012). Systematic social observation of children's neighborhoods using Google Street View: A reliable and cost-effective method. *Journal of Child Psychology and Psychiatry, 53*(10), 1009–1017.

Oke, T. R. (1981). Canyon geometry and the nocturnal urban heat island: Comparison of scale model and field observations. *Journal of Climatology, 1*(3), 237–254.

Otsu, N. (1975). A threshold selection method from gray-level histograms. *Automatica, 11*(285–296), 23–27.

Ratti, C., Di Sabatino, S., Britter, R., Brown, M., Caton, F., & Burian, S. (2002). Analysis of 3-D urban databases with respect to pollution dispersion for a number of European and American cities. *Water, Air, & Soil Pollution: Focus, 2*(5–6), 459–469.

Rundle, A. G., Bader, M. D., Richards, C. A., Neckerman, K. M., & Teitler, J. O. (2011). Using Google Street View to audit neighborhood environments. *American Journal of Preventive Medicine, 40*(1), 94–100.

Salesses, P., Schechtner, K., & Hidalgo, C. A. (2013). The collaborative image of the city: Mapping the inequality of urban perception. *PLoS ONE, 8*(7), e68400.

Svensson, M. K. (2004). Sky view factor analysis–implications for urban air temperature differences. *Meteorological Applications, 11*(03), 201–211.

Taylor, B. T., Fernando, P., Bauman, A. E., Williamson, A., Craig, J. C., & Redman, S. (2011). Measuring the quality of public open space using Google Earth. *American Journal of Preventive Medicine, 40*(2), 105–112.

Torii, A., Havlena, M., & Pajdla, T. (2009). From Google Street View to 3D city models. *IEEE 12th International Conference on Computer Vision Workshops* (pp. 2188–2195). Japan: Kyoto.

Unger, J. (2008). Connection between urban heat island and sky view factor approximated by a software tool on a 3D urban database. *International Journal of Environment and Pollution, 36* (1–3), 59–80.

Yang, J., Zhao, L., Mcbride, J., & Gong, P. (2009). Can you see green? Assessing the visibility of urban forests in cities. *Landscape and Urban Planning, 91*(2), 97–104.

Zamir, A. R., Darino, A., Patrick, R., & Shah, M. (2011). Street View challenge: Identification of commercial entities in Street View imagery. *Tenth International Conference on Machine Learning and Applications* (pp. 380–383). Hawaii, December: Honolulu.